Amina YACHIR[1], Houari Merabet BOULOUIHA[2], Abdallah BELABBES[3], Mohamed KHODJA[4] Riyadh BOUDDOU[5]

Laboratory of Automation and Systems Analysis LAAS, Ecole National Polytechnique Maurice Audin Oran, Algeria (1)
Laboratory of Sustainable Development of Electrical Energy LDDEE, University of Science and Technology MB Oran, Algeria(2)
University of Oran 2 Mohammed Ben Ahmed, Industrial maintenance and safety institute, Oran, Algeria (3)
University of Relizane Ahmed Zabana, Algeria (4)
Department of Electrical Engineering, Institute of Technology, University Center of Naama, Algeria (5)
ORCID: 1. 0009-0009-8156-0555; 2. 0000-0003-2218-8107; 3. 0000-0003-0072-6883; 5. 0000-0001-6555-5785

doi:10.15199/48.2024.09.15

Control Of a Grid-Connected PMSG-Based Wind Energy System with A Back-To-Back Converter Using a Hybrid Fuzzy Sliding Mode Control

Abstract. *Recently, the intersection of permanent magnet synchronous generator (PMSG)-based wind energy conversion system (WECS) has become a focus of research, stimulated by advances in advanced control techniques. This study explores the implementation of hybrid fuzzy sliding mode control in PMSG systems, with the aim of improving system response to varying wind conditions and enhancing overall stability and efficiency. By combining sliding mode control (SMC) with fuzzy logic control (FLC), this research contributes to the current discourse on the optimization of wind energy conversion systems. The obtained simulation outcomes of the proposed control strategy show robust dynamics, steady-state efficiency, and performance compared to conventional SMC and PI control, in terms of robustness and disturbances due to parameter variation.*

Streszczenie. *W ostatnim czasie system konwersji energii wiatrowej (WECS) oparty na generatorze synchronicznym z magnesami trwałymi (PMSG) stał się przedmiotem badań, stymulowanych postępem w zaawansowanych technikach sterowania. W niniejszym opracowaniu zbadano implementację hybrydowego sterowania rozmytego w trybie ślizgowym w systemach PMSG w celu poprawy reakcji systemu na zmienne warunki wiatrowe oraz zwiększenia ogólnej stabilności i wydajności. Łącząc sterowanie w trybie ślizgowym (SMC) ze sterowaniem logiką rozmytą (FLC), badania te przyczyniają się do obecnego dyskursu na temat optymalizacji systemów konwersji energii wiatrowej. Uzyskane wyniki symulacji proponowanej strategii sterowania pokazują solidną dynamikę, wydajność w stanie ustalonym i wydajność w porównaniu do konwencjonalnego sterowania SMC i PI, pod względem odporności i zakłóceń spowodowanych zmianami parametrów. (**Sterowanie systemem energetyki wiatrowej opartym na PMSG podłączonym do sieci z przetwornikiem typu back-to-back przy użyciu hybrydowego sterowania w trybie rozmytym)*

Keywords: WECS, PMSG, SMC, FLC
Słowa kluczowe: WECS, PMSG, SMC, FLC.

Introduction

In recent years, the intersection of PMSG-based wind energy conversion systems has emerged as a focal point of research, driven by the rapid advancements in advanced control [1]. This dynamic landscape has opened new avenues for exploration and inquiry, pushing the boundaries of our understanding and challenging conventional wisdom. Within this context, the present study delves into implementing the fuzzy sliding control in our PMSG system, a critical aspect that demands scholarly attention [2]. As the advanced controls used in this later continue to evolve, the need for innovative solutions to improve the generator's response to varying wind conditions and enhance the overall stability and efficiency of the WECS becomes increasingly apparent [3]. Our research aims to contribute to this ongoing discourse by combining the benefits of both FLC and SMC controls. The fuzzy system helps in adapting the SMC parameters based on the current operating conditions, making the control system more adaptive and robust to uncertainties. The significance of our work lies in its potential to improve the response time, reduce maintenance costs, and enhance our system efficiency [4]. The PMSG-based WECS system comprises two distinct components, as illustrated in Figure 1: The Synchronous Generator Side Converter (SGSC) and the Grid Side Converter (GSC). Various control methodologies have been proposed for regulating the bidirectional IGBT converter. Each control approach possesses unique characteristics. Among the conventional control strategies is the widely known Proportional-Integral-Derivative control (PID)[1]. However, PID control has limitations stemming from fixed control parameters, specifically the proportional, integral, and derivative gains. Moreover, it does not inherently consider the distinctive dynamics and attributes inherent to the controlled system. Consequently, this can result in suboptimal performance, particularly in intricate and nonlinear systems.

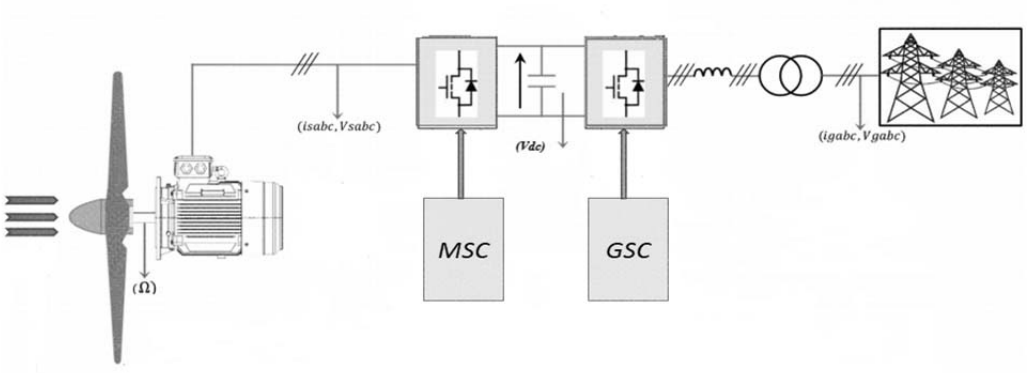

Fig.1. PMSG wind turbine control system

Conversely, advanced control techniques offer enhanced capabilities and address the challenges posed by nonlinear systems. Noteworthy options for linear systems include Field Oriented Control (FOC), FLC, SMC, and Fuzzy Sliding mode control (FSMC) [2]. These advanced methods exhibit a more comprehensive understanding of system dynamics, making them well-suited for optimizing the performance of PMSG-based WECS. This work is aimed to present FSMC for the control of the PMSG-based on wind energy [3].

This paper is structured as follows. In Section 2, the mathematical modeling of the generator and grid side of the PMSG wind turbine is discussed with the proposed maximum power point tracker (MPPT) control technique, while Sections 3 and 4 deal with the SMC technique and the model prediction technique, respectively. Section 5 discusses the simulation outcomes to compare and discuss the performance of the two advanced controls used.

Wind energy conversion system modeling

1. Wind generator modeling

The mechanical power $\boldsymbol{P_{tr}}$ obtained from the wind is written as, [5]

(1) $$P_{tr} = \frac{1}{2}\rho S v^3_{wind} C_p(\lambda,\beta)$$

The power coefficient $\boldsymbol{C_p(\lambda,\beta)}$ that represents the turbine's aerodynamic efficiency (which also relies on the speed ratio λ and the pitch angle) $\boldsymbol{\beta}$ is e given as: [6]

(2) $$\begin{cases} C_p(\lambda,\beta) = 0.5\left(\frac{116}{\lambda_i} - 0.4\beta - 5\right)e^{\frac{-21}{\lambda_i}} + 0.0068\lambda \\ \frac{1}{\lambda_i} = \frac{1}{\lambda + 0.08\times\beta} - \frac{0.035}{\beta^3+1} \\ \lambda = \frac{\Omega_{tr}.R}{v_{wind}} \end{cases}$$

The actual $\boldsymbol{C_p}$ curve of the wind turbine studied in this paper is illustrated in Figure 2. $\boldsymbol{C_p}$ is $\boldsymbol{C_{p-max} = 0.48}$ which corresponds to the blade orientation angle β = 0° and the optimal speed value ratio $\boldsymbol{\lambda_{opti} = 8.1}$. To extract the maximal energy generated, we need to set the speed ratio $\lambda optim$ and the maximal coefficient of power $\mathbf{C_{p-max}} = \mathbf{0.48}$.

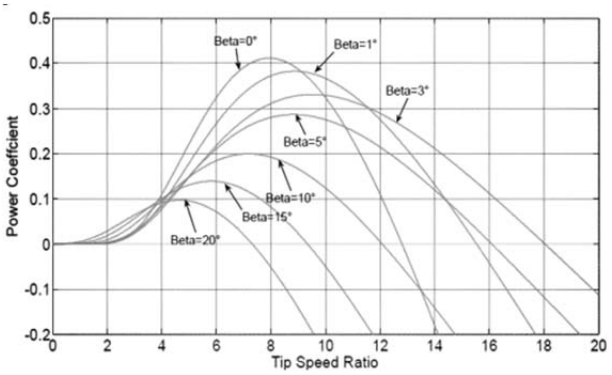

Fig. 2. Characteristic of coefficient.

$\boldsymbol{C_p} = (\boldsymbol{\lambda})$ as a function of the mechanical torque generated by the turbine is given by [7]:

(3) $$T_{tr} = \frac{P_{tr}}{\Omega_{tr}} = \frac{\rho\pi R^2 v^3_{vent} C_P(\lambda,\beta)}{2.\Omega_{tr}}$$

2. MPPT control technique

The proposed diagram shows a maximum power point tracking system with integral proportional control adapted to the PMSG at a wind turbine with variable speed. Figure 2 shows that $\boldsymbol{C_p}$ passes through a maximum for a particular value of the speed ratio that we call $\boldsymbol{\lambda_{opti}}$. For which we have maximum power coefficient $\boldsymbol{C_p}$, and consequently maximum captured power. It is then possible to develop control laws that get the maximal power whatever the wind speeds up to the rated power of the generator where the extracted power is limited to this value. [10]

Wind torque can be determined by estimating wind speed and measuring mechanical speed. [9]

(4) $$T^*_{tr\_opi} = \frac{P_{tr\_opti}}{\Omega} = \frac{1}{2.\Omega} C_{p\max}\left(\lambda_{opti},\beta\right).\rho.\pi.R^2\upsilon^3_{wind}$$

(5) $$T^*_{tr\_opi} = \frac{\rho\times\pi\times R^5\times C_{p-\max}\times\Omega_t^2}{2\times\lambda^3_{opt}}$$

Measuring the wind speed appearing at the turbine is tricky, but an estimate of its value can be obtained from the following equation. Figure 3 presents the wind turbine and MPPT model.

(6) $$\upsilon_{wimd\_ref} = \frac{\Omega\ .R}{\lambda_{opti}}$$

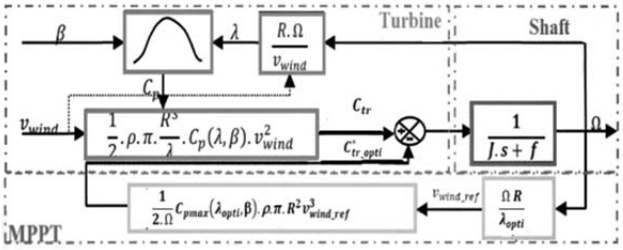

Fig. 3. Wind turbine and MPPT model.

3. Pitch Angle Control

The mechanism is used to rotate the blade approximately its longitudinal axis bodily. At better wind speeds, the torque or strength may be without problems confined to the nominal fee through adjusting the pitch attitude β. If the power is too high, the blade pitch mechanism is activated immediately, retaining the blades barely far from the wind [8]. Figure 4 presents the block diagram of the control system of the pitch angle.

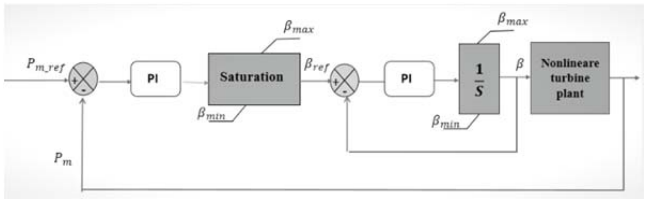

Fig. 4. Block diagram of the control system of the pitch angle.

4. PMSG Model

PMSG can be written, in the reference frame d-q with synchronous rotation, by the following system equation, [11]

- Stator Electric equations:

(7)
$$\begin{cases} \frac{dI_{sd}}{dt} = -\frac{R_s}{L_d} I_{sd} + \frac{\omega_s L_q}{L_d} I_{sq} + \frac{V_{sd}}{L_d} \\ \frac{dI_{sq}}{dt} = -\frac{R_s}{L_q} I_{sq} - \frac{\omega_s L_d}{L_q} I_{sd} - \frac{\omega_s \varphi_f}{L_q} + \frac{V_{sq}}{L_q} \end{cases}, \omega_s = P \times \Omega_{mec}$$

- Mechanical equations:

(8)
$$\begin{cases} T_{tr} - T_{em} = J.\frac{d\Omega_{mec}}{dt} - f_v.\Omega_{mec} \\ J = J_{tr} + J_g \end{cases}$$

The mechanical equation and the formula for the electromagnetic torque are given by the following equations: [9]:

(9)
$$T_{em} = \frac{3}{2} p\left((L_d - L_q) I_{sd} I_{sq} + \left(\varphi_f I_{sq}\right)\right)$$

(10)
$$\frac{d\Omega_{mec}}{dt} = \frac{1}{J}\left(T_{tr} - \left(\frac{3}{2} p \times \varphi_f \times I_{sq}\right) - f_v \Omega_{mec}\right)$$

5. Grid side model

The mathematical model of the GSC can be simplified by the following expression: [10]

(11)
$$\begin{cases} \frac{dI_{gd}}{dt} = \frac{V_{gd}}{L_f} - \frac{R_f}{L_f} I_{gd} + \omega_g I_{gq} - \frac{U_{gd}}{L_f} \\ \frac{dI_{gq}}{dt} = \frac{V_{gq}}{L_f} - \frac{R_f}{L_f} I_{gq} - \omega_g I_{gd} - \frac{U_{gq}}{L_f} \end{cases}$$

Where V_{gd} and V_{gq} are the components of the d-q axis voltage of the inverter, and L_f and R_f are respectively the grid side filter inductance and resistance, connected in series, and U_{gd} and U_{gq} are the output voltage of the converter in the d-q frame. The stator active and reactive outputs are given by:

(12)
$$\begin{cases} P_g = \frac{3}{2}\left(V_{gd} I_{gd} + V_{gq} I_{gq}\right) \\ Q_g = \frac{3}{2}\left(V_{gq} I_{gd} - V_{dq} I_{gq}\right) \end{cases}$$

3. Wind energy system control Strategies

1. Theory of SMC

The SMC technique is a special control system with a variable structure. Its principle is to force the system state trajectory towards a sliding surface and to make it evolve in the vicinity of the surface, with a certain dynamic to the equilibrium point, through an appropriate switching logic [13-14]. The general equation, proposed by [19], to determine the sliding surfaces and to ensure the convergence of the variables to the desired value is as follows:

(13)
$$S(x) = \left(\frac{d}{dt} + \lambda\right)^{r-1} e(x) \qquad (\lambda > 0)$$

Where *r* represents the system order, λ is a constant and $e(x)$ is the error from the state variable to the desired signal.

If *r* = 1 is chosen, the dynamics of the proposed sliding surface tracking error is as follows:

(14)
$$S(X) = e(t) = X^* - X$$

The control law is obtained by adding two terms, such that [12] [13]:

(15)
$$u_{smc} = u_{equ} + u_n$$

u_{equ} is the equivalent control, a low-frequency term influencing the mode of approach mode to reach the sliding surface u_n is the non-linear control, a discontinuous high-frequency term influencing the sliding mode by keeping the system on the general form of discontinuous control is the

(16)
$$u_n = k.sign\left[S(x)\right]$$

k is a diagonal matrix with constant positive coefficients and allows for adjustment of the desired dynamics [16] [17]. $sign\left[S(x)\right]$ is a mathematical function with an incomplete switching function that results in a chattering control signal. This behaviour, called chattering, causes high-frequency oscillations due to control frequency oscillations due to control discontinuities. It can deteriorate the system by exciting dynamics neglected in the modelling or damage the actuators by too frequent stresses. To minimize this effect, a novel continuous smooth switching control is proposed to achieve smoothing of the signal. The concept of this technique is to replace the ordinary discrete function (sign) in the switching control with a continuous smooth function, as follows [14] [15]:

(17)
$$u_n = k.Smooth\left[S(x)\right]$$

Where $Smooth\left[S(x)\right]$ is a function that is smooth and continuous, given by [20]:

(18)
$$smooth\left[\lambda', S\right] = \frac{\lambda' S}{\left|\lambda' S\right| + \varepsilon}$$

ε is a positive small of the limit layer width and λ' is a constant for adjusting the function's tuning rate. The two parameters (λ', ε) define the slope of the continuous function. In addition, the state-dependent limit layer ε is constructed as follows:

(19)
$$\varepsilon = \left(1 - \left|smooth\left[\lambda', S\right]\right| + \delta_1\right)$$

Where δ_1 is a small positive constant

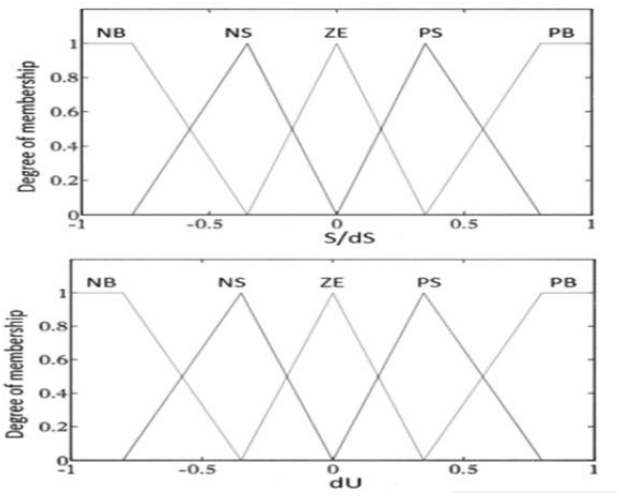

Fig.5. The membership functions

3.2 Design and modeling of FLC controller

One of the well-known drawbacks of SMC is the chattering effect. In this part, FLC control is implemented to

solve this problem, the state trajectory can reach and move along the change surface, and a good dynamic steady state can be
achieved by combining SMC and FLC. Figure 5 presents the membership functions [11],[14]

Table 1. Matrix of Inference

$dU_{1,2}$		$dS_{1,2}$				
		NB	**NS**	**ZE**	**PS**	**PB**
$S_{1,2}$	**NB**	NB	NB	NS	NS	ZE
	NS	NB	NS	NS	ZE	PS
	ZE	NS	NS	ZE	PS	PS
	PS	NS	ZE	PS	PS	PB
	PB	ZE	PS	PS	PB	PB

With, NB: Negative Big, NS: Negative Small, ZE: Equal Zero, PS: Positive Small, PB: Positive Big.

3.3 Design and modelling of the FSMC

The conventional SMC is designed on the basis of the discrete function of the system state variables that are used to generate a " sliding surface ". Once this surface is attained, the discrete function maintains the trajectory on the surface such that the required system dynamics are achieved [18]. In this work, the controllers are replaced by an FSMC to obtain reliable performance. By keeping part of the equivalent control SMC and introducing the FLC, a new control approach FSMC is obtained, as presented in Figure 6 [22].

(20) $$u_{FSMC} = u_{equ} + u_f$$

The two components are combined to ensure the system's stability and robustness.

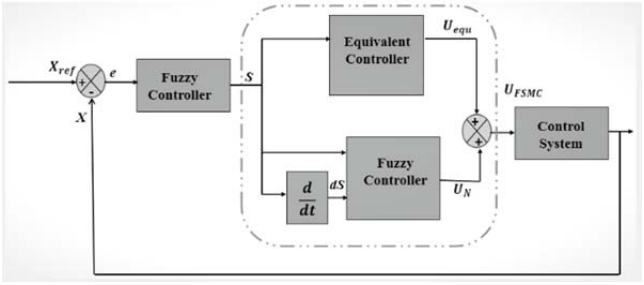

Fig.6. The structure diagram of the hybrid control FSMC

3.1 MSC model in synchronous generator side converter control

Figure 7 depicts the proposed MSC control scheme. The hybrid control FSMC bloc is detailed in Fig. 6.

We have three controllers, that are designed to control the d-q axis stator current (I_{sd}, I_{sq}) and the speed (Ω_{mec})in this side The sliding surfaces have been fixed as follows [21]:

(21) $$S(I_{sd}) = e(I_{sd}) = I_{sd}^* - I_{sd}$$

(22) $$S(I_{sq}) = e(I_{sq}) = I_{sq}^* - I_{sq}$$

(23) $$S(\Omega_{mec}) = e(\Omega_{mec}) = \Omega_{mec}^* - \Omega_{mec}$$

Whit I_{sd}^* and I_{sq}^* are the dq axis reference stator current respectively

Each axis control is as follows [6]:

(24) $$V_{sd_{ref}} = V_{sd_{eq}} + V_{sd_N}$$

(25) $$V_{sq_{ref}} = V_{sq_{eq}} + V_{sq_N}$$

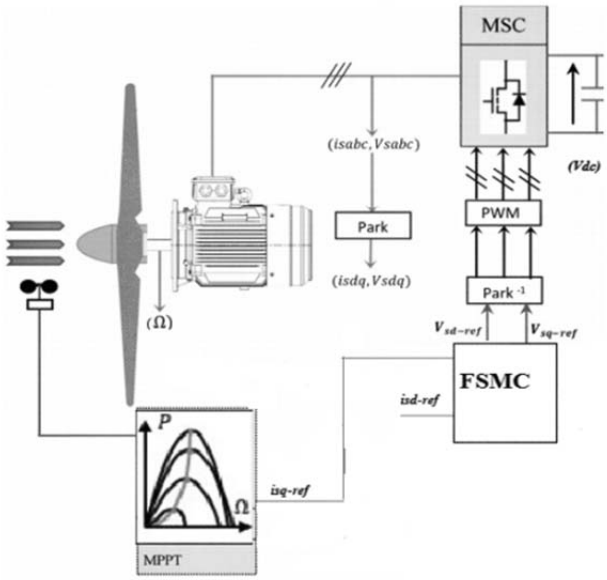

Fig.7. Generator side of PMSG wind turbine control system

By applying the time derivative to expressions (7) and taking into account that the sliding mode occurs on the sliding surface when $(\dot{S}(x) = 0)$, therefor we obtain the following control equations:

(26) $$V_{sd_{eq}} = L_d[\frac{dI_{sd}^*}{dt} + \frac{R_s}{L_d} I_{sd} - \omega_s \frac{L_q}{L_d} I_{sq}]$$

(27) $$V_{sq_{eq}} = L_q[\frac{dI_{sq}^*}{dt} + \frac{R_s}{L_q} I_{sq} + \omega_s \frac{L_d}{L_q} I_{sd} + \omega_s \frac{\varphi_f}{L_q}]$$

With the switching control expressions are defined as follows:

(28) $$V_{sd_N} = K_{gd} \times smooth\left(S(I_{sd})\right) \text{ with } K_{sd} > 0$$

(29) $$V_{sq_N} = K_{gq} \times smooth\left(S(I_{sq})\right) \text{ with } K_{sq} > 0$$

The d-axis stator current is maintained at zero to obtain maximum torque and the q-axis stator current is controlled using the sliding mode:

(30) $$I_{sq}^* = I_{sq_{eq}} + I_{sq_N}$$

We apply the derivative to equation (10) to obtain the following control expression:

(31) $$I_{sq_{eq}} = -\frac{2J}{3p\varphi_f}[\frac{d\Omega_{mec}^*}{dt} + \frac{f_v}{J}\Omega_{mec} - \frac{1}{J}T_{tr}]$$

With,

(32) $$I_{sq_N} = K_{\Omega_{mec}} \times smooth\left(S(\Omega_{mec})\right) \text{ with } K_{\Omega_{mec}} > 0$$

Where Ω_{mec}^* is the mechanical speed reference.

2 GSC Control

On this side, using SMC mode, two controllers are designed to control the d-q axis grid current (i_{gd}, i_{gq}),as shown in Figure 9 with the overall GSC diagram in Figure 8. [22] [23]

The sliding surfaces are defined as follows [10]:

(33) $$S(I_{gd}) = e(I_{gd}) = I_{gd}^* - I_{gd}$$

(34) $$S(I_{gq}) = e(I_{gq}) = I_{gq}^* - I_{gq}$$

Each axis control is as follows [6]:

(35) $$V_{gd_{ref}} = V_{gd_{eq}} + V_{gd_N}$$

(36) $$V_{gq_{ref}} = V_{gq_{eq}} + V_{gq_N}$$

We apply the time derivative to expressions (11):

(37) $$V_{gd_{eq}} = L_f\left[\frac{dI^*_{gd}}{dt} + \frac{R_f}{L_f} I_{gd} - \omega_g I_{gq} + \frac{U_{gd}}{L_f}\right]$$

(38) $$V_{sq_{eq}} = L_f\left[\frac{dI^*_{gq}}{dt} + \frac{R_f}{L_f} I_{gq} + \omega_g I_{gd} + \frac{U_{gq}}{L_f}\right]$$

The switching control expressions are defined as:

(39) $$V_{gd_N} = K_{gd} \times smooth\left(S(I_{gd})\right) \text{ with } K_{gd} > 0$$

(40) $$V_{gq_N} = K_{gq} \times smooth\left(S(I_{gq})\right) \text{ with } K_{gq} > 0$$

With i^*_{gd} and i^*_{gq} are the d-q axis reference grid current respectively, the d-axis grid current is controlled using an external PI controller that regulates the voltage measured in DC-link to track its reference at a constant value, and the q-axis grid current is controlled also with an external PI controller that regulates the reactive power to its reference that is fixed at zero to reach the unity power factor.

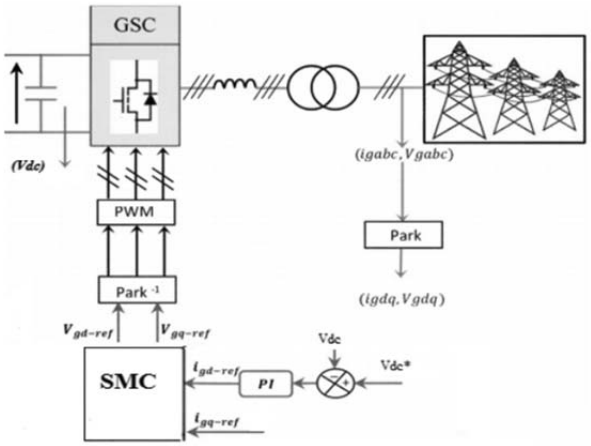

Fig.8. Grid side PMSG wind turbine control system

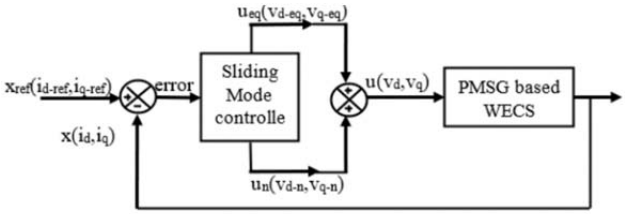

Fig.9. The overall structure of the SMC.

5. Simulation results

To evaluate the performances of the three control strategies FSMC and SMC-PI, we performed a test in MATLAB/Simulink of the behaviour of the PMSG-based wind system in a dynamical regime, where the turbine is operated by a wind speed that varies using the MPPT approach to approximate reality Figure 10. The parameters of the wind system and the basic simulation parameters are shown in Table 2, table 3, table 4 and table 5. The simulation results are presented in Figure 11, Figure 12, Figure 13, Figure 14,

Figure 14, Figure 15, Figure 16, Figure 17, and Figure 18.

Table 2. Parameters of PMSG

Symbol	Value
Rated power P_m	2 MW
Nominal voltage	5000 V
Stator resistance R_s	0.00625 Ω
Stator direct inductance L_{sd}	0.004229 H
Stator quadrature inductance L_{sd}	0.004229 H
The moment of inertia J	10000 $Kg.m^2$
The friction coefficient f	0.0142 $N.m$
Pole pairs P	75

Table 3. Parameters of wind turbine

Symbol	Value
Blade length R	55 m
Air density ρ	1.225 Kg/m^3
Gain multiplier G	1

Table 4. Parameters of the grid

Symbol	Value
Filter resistance R_f	0.002 Ω
Filter inductance L_f	0.004 H
Fixed-step size T_s	1e-5

Table 5. Parameters of SMC

Symbol	Value
Gain K_{mec}	7000
Gain K_{sd}	20
Gain K_{sq}	30
Gain K_{gd}	100
Gain K_{gq}	300

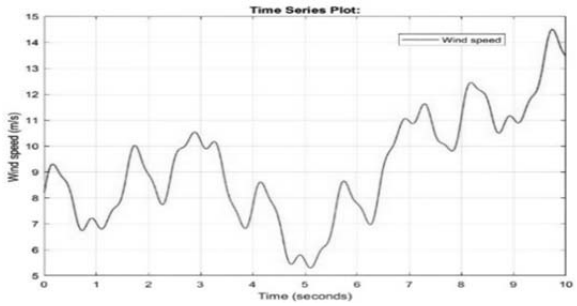

Fig.10. Wind speed characteristics

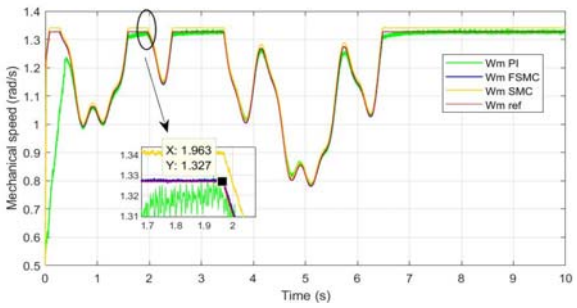

Fig.11. Mechanical speed.

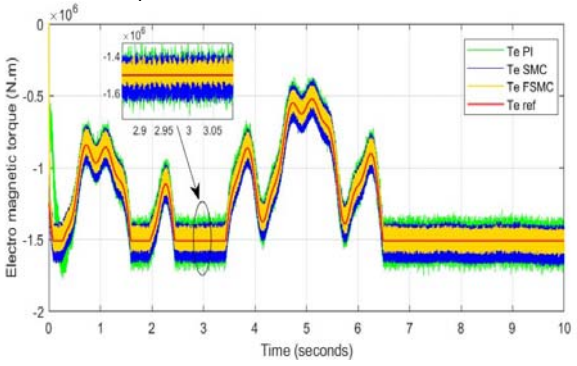

Fig.12.Electromagnetic torque

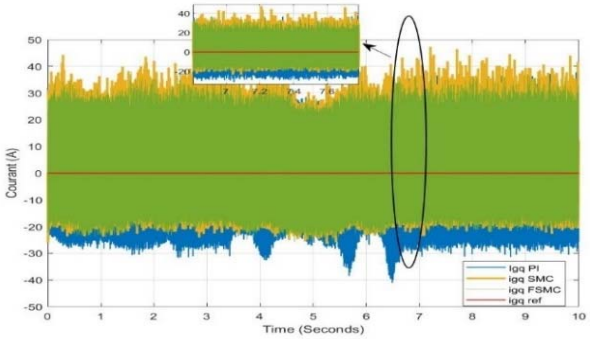

Fig.13.Grid current of SMC

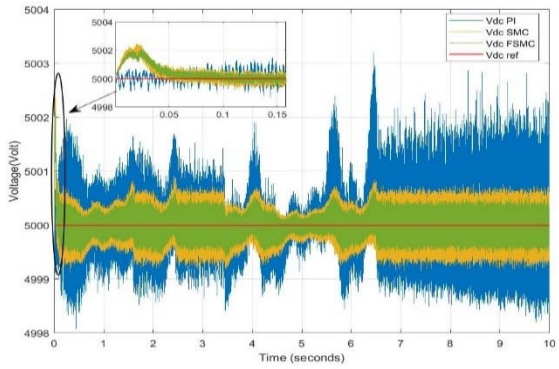

Fig.14. DC bus voltage.

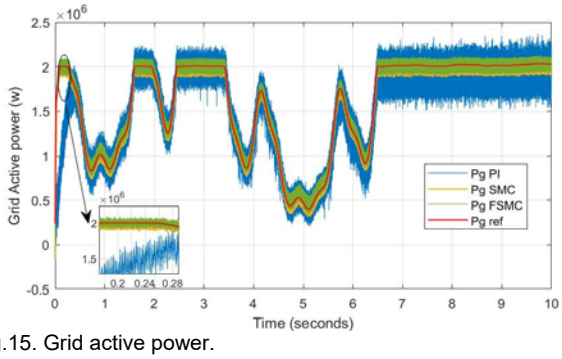

Fig.15. Grid active power.

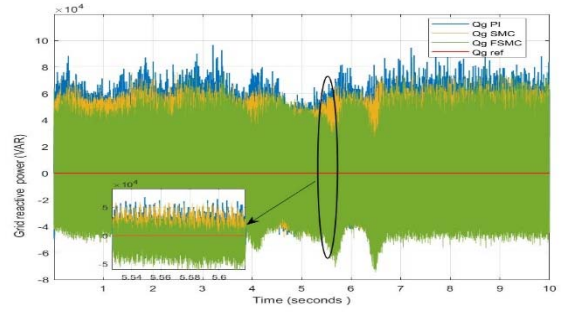

Fig.16. Grid reactive power.

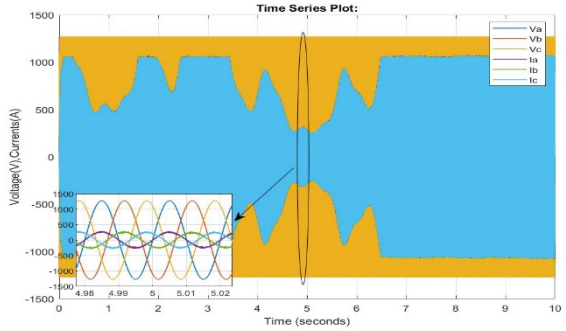

Fig.17. Voltage and injected current using the FSMC strategy

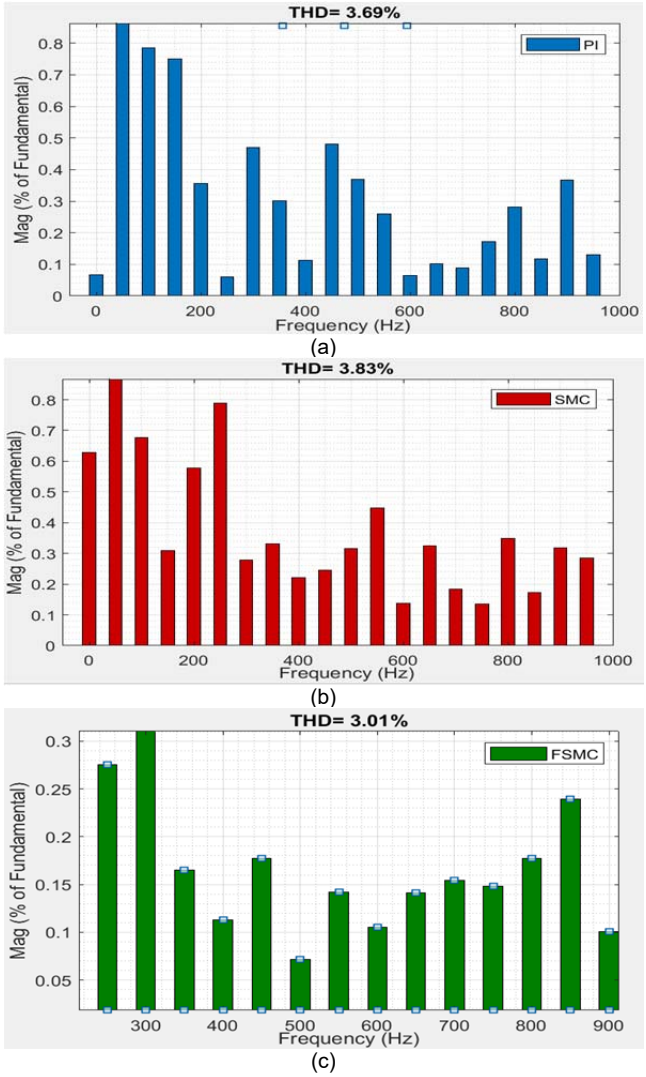

Fig.18. (a) THD using CSMC and (b) THD using PSMC

On all three graphs Fig.11.12.13, the hybrid FSMC control demonstrates superior accuracy compared to conventional SMC and PI controls. In addition, the FSMC curves exhibit smoother behavior, eliminating chatter phenomena, thus indicating its improved performance in terms of stability precision and speed. Figure 14 shows that the DC-link voltage is maintained constant and follows accurately the reference value as it should be. In Figure 15 and Figure 16, the powers follow their reference values in infinite time with good accuracy and respected decoupling (the active power is negative, which means that the PMSG operates as a generator). The amplitudes of FSMC and SMC ripples are smaller and occur in a shorter period than the obtained for the PI controller. Network currents and voltages are sinusoidal with a frequency of 50 Hz and their amplitudes vary with the variation in wind speed, as shown in fig.17.

Furthermore, it is essential to carry out a harmonic analysis to verify that the THD of the injected current is within the IEEE limit (THD ≤ 5%). Figure 18 shows that the total THD obtained by the FSMC (THD = 3.01%) is significantly lower than the THD obtained by the SMC and PI (THD = 3.83%, THD = 3.69%).

6. Conclusion

In this paper, a hybrid FSMC strategy is proposed for a PMSG generator with variable wind speed. The control performance was investigated in the MATLAB/Simulink

environment. The results of the simulation and the comparative study confirmed that the proposed control is more relevant for WECS systems based on the PMSG, the robustness and the accuracy of the reference tracking are improved with the hybrid fuzzy sliding mode approach as well as its capability to minimize the chattering effect.

Authors

***Mr. Amina YACHIR**, Laboratory of Automation and Systems Analysis LAAS, Ecole National Polytechnique Maurice Audin Oran, Algeria, amina.inge@yahoo.fr.*

***Prof. Houari Merabet BOULOUIHA**, Laboratory of Sustainable Development of Electrical Energy LDDEE, University of Science and Technology MB Oran, Algeria, E-mail: houari.merabet@gmail.com.*

***Dr. Abdallah BELABBES**,* University of Science and Technology MB, Laboratory of Vision Automation and Intelligent Control Systems AVCIS, Bir El Djir, 31000 Oran, Algeria E-mail: abdallah.belabbes@gmail.com.

***Dr. Mohamed KHODJA**, University of Relizane Ahmed Zabana, Algeria,* E-mail: khodja1970@gmail.com

***Dr. Riyadh BOUDDOU**, IEEE Member, Departement of Electrical Engineering, Institute of Technology, University Center of Naama, Algeria, IRECOM Laboratory, E-mail: bouddou@cuniv-naama.dz, riyadh.bouddou@ieee.org.*

REFERENCES

[1] YANG, Bo, YU, Tao, SHU, Hongchun, et al. Adaptive fractional-order PID control of PMSG-based wind energy conversion system for MPPT using linear observers. International Transactions on Electrical Energy Systems, 2019, vol. 29, no 1, p. e2697.

[2] NARAYANAN, G., ALI, M. Syed, JOO, Young Hoon, et al. Robust Adaptive Fractional Sliding-Mode Controller Design for Mittag-Leffler Synchronization of Fractional-Order PMSG-Based Wind Turbine System. IEEE Transactions on Systems, Man, and Cybernetics: Systems, 2023.

[3] LI, Yujun, XU, Zhao, et WONG, Kit Po. Advanced control strategies of PMSG-based wind turbines for system inertia support. IEEE Transactions on Power Systems, 2016, vol. 32, no 4, p. 3027-3037.

[4] BENAMOR, A., BENCHOUIA, M. T., SRAIRI, K., et al. A novel rooted tree optimization applies in the high order sliding mode control using super-twisting algorithm based on DTC scheme for DFIG. International Journal of Electrical Power & Energy Systems, 2019, vol. 108, p. 293-302.

[5] Achar, A., Djeriri, Y., Bentaallah, A., Hanafi, S., Djehaf, M. A., & Bouddou, R. (2023). Lyapunov-based robust power controllers for a wind farm using parallel multicell converters. Przegląd Elektrotechniczny, 99(4), 247-254.

[6] KALI, Syed Wajahat, VERMA, Anant Kumar, TERRICHE, Yacine, et al. Finite-Control-Set Model Predictive Control for Low-Voltage-Ride-Through Enhancement of PMSG Based Wind Energy Grid Connection Systems. Mathematics, 2022, vol. 10, no 22, p. 4266.

[7] K ABDELLATIF, Walid SE, HAMADA, A. M., et ABDELWAHAB, Saad A. Mohamed. Wind speed estimation MPPT technique of DFIG-based wind turbines theoretical and experimental investigation. Electrical Engineering, 2021, p. 1-13.

[8] REZAEI, Najmeh, MEHRAN, Kamyar, et COSSAR, Calum. A practical model and an optimal controller for variable speed wind turbine permanent magnet synchronous generator. In: 2017 9th International Conference on Modelling, Identification and Control (ICMIC). IEEE, 2017. p. 1008-1013.

[9] KESRAOUI, Mohamed, LAGRAF, Sid Ahmed, et CHAIB, Ahmed. Aerodynamic power control of wind turbine using fuzzy logic. In: 2015 3rd international renewable and sustainable energy conference (IRSEC). IEEE, 2015. p. 1-6.

[10] MEGHNI, Billel, DIB, Djalel, et AZAR, Ahmad Taher. A second-order sliding mode and fuzzy logic control to optimal energy management in wind turbine with battery storage. Neural Computing and Applications, 2017, vol. 28, p. 1417-1434.

[11] GHOURAF, Djamel Eddine. An advanced control applied to PMSG wind energy conversion system implemented under graphical user interface. Electrical Engineering, 2023, p. 1-12.

[12] OTHMANE, Zamzoum, et al. Dynamic modeling and control of a wind turbine with MPPT control connected to the grid by using PMSG. In: 2017 International conference on advanced technologies for signal and image processing (ATSIP). IEEE, 2017. p. 1-6.

[13] YIN, Xiu-xing, LIN, Yong-gang, LI, Wei, et al. A novel fuzzy integral sliding mode current control strategy for maximizing wind power extraction and eliminating voltage harmonics. Energy, 2015, vol. 85, p. 677-686.

[14] ZRIBI, Mohamed, ALRIFAI, Muthana, et RAYAN, Mohamed. Sliding mode control of a variable-speed wind energy conversion system using a squirrel cage induction generator. Energies, 2017, vol. 10, no 5, p. 604.

[15] RHAILI, S. E., ABBOU, A., HICHAMI, N. E., et al. Mawimum power extraction of five-phase PMSG WECS by adopting and improved fractional order sliding mode strategy. Jilin DaxueXuebao, 2021, p. 55-74.

[16] MAJOUT, Btissam, BOSSOUFI, Badre, BOUDERBALA, Manale, et al. Improvement of PMSG-based wind energy conversion system using developed sliding mode control. Energies, 2022, vol. 15, no 5, p. 1625.

[17] Belabbes, A., Hamane, B., Bouhamida, M., & Draou, A. (2012). Power control of a wind energy conversion system based on a doubly fed induction generator using RST and sliding mode controllers. RE&PQJ, 10(2).

[18] ECHIHEB, Farah, IHEDRANE, Yasmine, BOSSOUFI, Badre, et al. Robust sliding-backstepping mode control of a wind system based on the DFIG generator. Scientific reports, 2022, vol. 12, no 1, p. 11782.

[19] JUNHUI, Zhao, MINGYU, Wang, YANG, Li, et al. The study on the constant switching frequency direct torque-controlled induction motor drive with a fuzzy sliding mode speed controller. In: 2008 International Conference on Electrical Machines and Systems. IEEE, 2008. p. 1543-1548.

[20] AISSAOUI, Abdel G., ABID, H., et ABID, M. Robust fuzzy sliding mode controller design for motors drives. Acta Electrotechnica et Informatica, 2009, vol. 9, no 2, p. 64-71

[21] Azzouz, S., Messalti, S., & Harrag, A. (2019). Innovative PID-GA MPPT controller for extraction of maximum power from variable wind turbine. Przegląd Elektrotechniczny, 95.

[22] ABDELGOUI, Rim Feyrouz, TALEB, Rachid, BENYOUCEF, Djilali, et al. A Comparative Study Between Sliding Mode Control (SMC) and Hybrid Control Fuzzy Sliding Mode (FSMC) for Induction Motor. In: Second International Conference on Electrical Engineering ICEEB'18. 2018.

[23] BELABBES, A, LAIDANI, A, YACHIR A, BOUZID, A, E, LITIM, O, A, BOUDDOU, R. (2024). Advanced Control of PMSG-based Wind Energy Conversion System Using Model Predictive and Sliding Mode Control. PRZEGLĄD ELEKTROTECHNICZNY, 1(2), 12–18. https://doi.org/10.15199/48.2024.02.02